Celal Bayar University Journal of Science
Volume 22, Issue 2, 2026, p 320-326
Doi: 10.18466/cbayarfbe.1837651
Research Article

Celal Bayar University Journal of Science

New Fluorinated Phenoxy-Containing Zinc (II) Phthalocyanine; Synthesis, Aggregation Behavior, and Singlet Oxygen Production Capacity

Nazli Farajzadeh Öztürk[1]*, Sevgi Sarıgül Özbek[1]

[1] Department of Analytical Chemistry, Faculty of Pharmacy, Acıbadem Mehmet Ali Aydınlar University, İstanbul, Türkiye
* nazli.ozturk@acibadem.edu.tr
* Orcid No: 0000-0002-3857-5673

Received: December 7, 2025
Accepted: March 11, 2026
DOI: 10.18466/cbayarfbe.1837651

Abstract

Photodynamic therapy has been considered a suitable alternative to chemotherapy in recent years. In this method, a photosensitizing agent is activated by light, converting triplet oxygen molecules into singlet oxygen, which is required for the elimination of cancerous tissues. This study reports the synthesis of a new phthalonitrile derivative (1), namely 4-chloro-5-(4-(trifluoromethoxy)phenoxy)phthalonitrile. Its structural characterization was performed using ^{1}H nuclear magnetic resonance (NMR) and Fourier transform infrared (FT-IR) spectroscopy. Zinc (II) phthalocyanine (ZnPc) was synthesized by cyclotetramerization of compound (1) in the presence of the zinc ion. Its characterization was performed using ^{1}H NMR, FT-IR, matrix-assisted laser desorption/ionization time-of-flight (MALDI-TOF), and ultraviolet-visible (UV-vis) spectroscopy. The electronic absorption spectra of the macromolecule (ZnPc) were recorded at different concentrations in various solvents to study the effects of concentration and solvent nature on its aggregation behavior. The efficiency of zinc (II) phthalocyanine in photodynamic therapy was evaluated by measuring its singlet-oxygen quantum yield. The macromolecule exhibited high solubility at the studied concentration in ethanol, dichloromethane, and dimethyl sulfoxide. Additionally, its singlet-oxygen quantum yield was calculated to be 0.81, higher than that of the unsubstituted zinc (II) phthalocyanine.

Keywords: Phthalocyanine, Fluorine, Singlet oxygen, Aggregation

1. Introduction

Phthalocyanines are well-known porphyrin analogs that contain four indole units. Their planar 18π-electron structure gives rise to intense electronic transitions, which in turn yield unique electronic, optical, and chemical properties. Hence, the potential of phthalocyanines has been studied in various scientific and high-tech areas, including photodynamic therapy (PDT) [1], nonlinear optics (NLO) [2], sensors [3], nanotechnology [4], catalysts [5], etc. However, their poor solubility in most organic solvents and in aqueous media is a fundamental drawback that limits their utility in many applications. Alteration of the phthalocyanine periphery and/or insertion of metal ions into the core of the phthalocyanine ring can improve the solubility. These structural changes can also refine the electrical and optical characteristics of phthalocyanines [1-8]. As phthalocyanines are irradiated at the UV-vis range, their excited population increases and is then quenched in various ways. Therefore, the design of reactions by effectively leveraging the optical properties of phthalocyanines will be feasible for many photonic and radiosensitizing applications in ecology, electronics, medicine, and chemical technology. Generally, the stability of metal phthalocyanines depends on the metal ion, solvent type, the reducers and/or oxidants. Since phthalocyanine molecules excited by radiation can decompose, particularly in the presence of oxygen or other radical-generating species, this parameter is considered a limiting factor, but it occurs infrequently [9].

The presence of bulk and long phenoxy groups significantly increases the solubility of phthalocyanines in organic solvents. Additionally, phenoxy-containing phthalocyanines exhibit excellent optical and biological properties, including high fluorescence, efficient singlet-oxygen generation, and a large Stokes shift [10,11]. On

the other hand, fluorine is the most electronegative element, which can confer extraordinary chemical, biological, and physical properties when incorporated into a structure. Replacing a fluorine atom in a hydrocarbon with a proton increases its reactivity. Indeed, coulombic interactions between fluorine and the carbon formed by the polarized covalent bond lead to a very strong carbon-fluorine bond [12]. Its high polarization enhances the solubility, reactivity, and stability of fluorinated compounds relative to non-fluorinated compounds [13]. On the other hand, the insertion of metal ions into the phthalocyanine ring can improve the solubility of phthalocyanines and their electronic properties. Additionally, metallic centers can confer specific properties on phthalocyanines. For instance, zinc ions are approximately not toxic in low amounts (<225 mg); therefore, zinc (II) phthalocyanines can be utilized in many biomedical applications. Since the d^{10} configuration of the zinc (II) ion makes its direct contribution to the electronic spectra of phthalocyanines, the structure and electronic properties of the zinc (II) can be anticipated reliably to design new photosensitizing agents. Due to the suitable size of the zinc ion (0.88 Å), it is usually kept tightly in the center of the phthalocyanine ring without destruction of its two-dimensional structure [14]. Nonplanarity of some metal phthalocyanines is usually assigned to the oxidation state of the metal cation.

In this study, a novel fluorinated phthalonitrile was synthesized and used to prepare a new zinc (II) phthalocyanine derivative, which can be considered an efficient photosensitizing agent for photodynamic therapeutic applications. The aggregation behavior of the newly synthesized phthalocyanine was examined at different concentrations and in various solvents. Additionally, its potential for singlet oxygen generation was studied by calculating the related quantum yield.

2. Materials and Methods

2.1 Equipment

A PerkinElmer Spectrum One spectrometer (4000–400 cm^{-1}), an Agilent VNMRS 500 MHz spectrometer, a Scinco Lab Pro Plus UV/Vis spectrophotometer, and a Bruker Microflex MALDI–TOF mass spectrometer were used to record FT-IR, ^{1}H NMR, electronic absorption, and mass spectra of the newly synthesized compounds, respectively.

2.2 Synthesis and Characterization

2.2.1 Phthalonitrile derivative 1

4,5-dichlorophthalonitrile (1.00 g, 5.08 mmol) and 4-trifluoromethoxyphenol (0.99 g, 5.60 mmol) were dissolved in dry N,N-dimethylformamide (DMF; 10 mL). Potassium carbonate (1.40 g, 10.11 mmol) was added to the mixture. The reaction mixture was stirred at room temperature for 48 hours. Then, the mixture was treated with iced water (50 mL), stirred for 1 hour, and filtered off. The phthalonitrile derivative was purified by crystallization from ethanol. Molecular formula: $C_{15}H_6ClF_3N_2O_2$. Yield: 1.23 g (71.5%). ^{1}H NMR (500 MHz; DMSO-d_6): δ 8.26 (s, 1H), 8.09 (s, 1H), 7.87-7.82 (bd, 2H), 7.44-7.34 (bd, 2H) ppm. FT-IR υ (cm^{-1}): 3082 (aromatic C–H), 2259 (nitrile C≡N), 1387 (CF_3), 1086 (C-O-C). ^{13}C NMR (126 MHz; DMSO-d_6): δ 152.44, 151.34, 146.47, 146.46, 123.45, 123.28, 122.82, 121.57, 121.40, 120.70, 119.35, 117.30, 114.60, 111.36 ppm.

2.2.2 Zinc (II) phthalocyanine (ZnPc)

Compound 1 (0.10 g, 0.30 mmol) and zinc acetate (0.015 g, 0.081 mmol) were dissolved in 3 mL 2-dimethylaminoethanol (DMAE) for 24 hours at reflux temperature under nitrogen. After cooling to room temperature, the mixture was treated with an ice-water mixture. The crude material was precipitated, filtered, and dried in an oven. The product was purified by column chromatography on silica gel using chloroform: tetrahydrofuran as the mobile phase. Molecular formula: $C_{60}H_{24}Cl_4F_{12}N_8O_8Zn$. Yield: 0.060 g (57%). ^{1}H NMR (500 MHz; DMSO-d6): δ 8.10 (s, 1H), 7.78 (s, 1H), 7.60-7.55 (bd, 2H), 7.35-7.31 (bd, 2H) ppm. FT-IR υ (cm^{-1}): 3069 (C–H aromatic), 1379 (CF_3), 1082 (C-O-C). MS m/z calcd. 1420.05 $[M]^+$ found 1437.39 $[M + OH]^+$.

2.3 Aggregation Studies

The aggregation behavior of ZnPc was studied at concentrations ranging from 1 to 20 µM. To prepare a stock solution of ZnPc, 2.84 mg of the phthalocyanine was dissolved in sufficient dimethyl sulfoxide (DMSO) to bring the final volume to 100 mL. The same procedure was used to prepare stock solutions of dichloromethane (DCM) and ethanol. The samples used for aggregation studies were prepared by diluting the corresponding stock solution (20 µM).

2.4 Singlet Oxygen Quantum Yield (ϕ_Δ)

The capacity of ZnPc to produce singlet oxygen was measured by studying the phosphorescence of $^1O_2$. A Horiba–Jobin–Yvon Fluorimeter with a Hamamatsu NIR PMT 5509 was used [15], and the ϕ_Δ value of ZnPc was calculated by performing equation (1):

$$\phi_\Delta = \phi_\Delta(std)\left(\frac{I_\Delta \,.\, A(std)}{I_\Delta(std) \,.\, A}\right) \qquad (1)$$

where ϕ_Δ (std), I_Δ, and A are the singlet oxygen quantum yield of the standard (unsubstituted zinc (II) phthalocyanine; ϕ_Δ = 0.67 in DMSO), the area under the curve of the peak of singlet oxygen at 1206 nm, and the absorbance, respectively.

3. Results and Discussion

3.1 Synthesis and Characterization

The synthetic route for compound (1) is portrayed in Scheme 1. Phthalonitrile derivative (1) was synthesized via an aromatic substitution of the hydroxy group of 4-trifluoromethoxyphenol with a chlorine atom of 4,5-dichlorophthalonitrile. The compound was purified by recrystallization from ethanol, and its structure was characterized using ^{1}H and ^{13}C NMR and FT-IR spectroscopy. The results were in accordance with the predicted structure. In the reactants and the product (1), only aromatic protons are present, and their chemical shifts are similar in the aromatic region. Therefore, they may not be differentiated, and the expected signals for the aromatic H's appeared in the ^{1}H NMR spectrum of compound 1. However, the absence of the OH signal, which is usually seen as a broad singlet, is a clear indication of the formation of the product. In the ^{1}H NMR spectrum of compound 1, the signals of aromatic protons observed at 8.26 (1H) and 8.09 (1H) as singlets were assigned to the protons of the phthalonitrile, whereas those appearing around 7.87-7.82 (2H) and 7.44-7.34 (2H) as broad doublets corresponded to the protons of the 4-trifluoromethoxyphenyl group. In the ^{13}C NMR of compound 1, the carbon atoms of the phenyl rings appeared between 152.44 and 111.36 ppm. The carbons bonded to the halogens appeared at around 123 ppm due to inductive of the chlorine, which decreases the local electron density and leads to deshielding of the attached carbon atoms, whereas those of the nitriles were observed at 121.57 and 121.40 ppm. This relatively upfield position of the nitrile carbons can be attributed to their sp-hybridized nature and high s-character, which leads to increased shielding despite the cyano group being strongly electron-withdrawing. In the FT-IR spectrum of compound 1, the bands that were observed at 3082, 2259, 1387, and 1086 cm^{-1} were attributed to the C-H

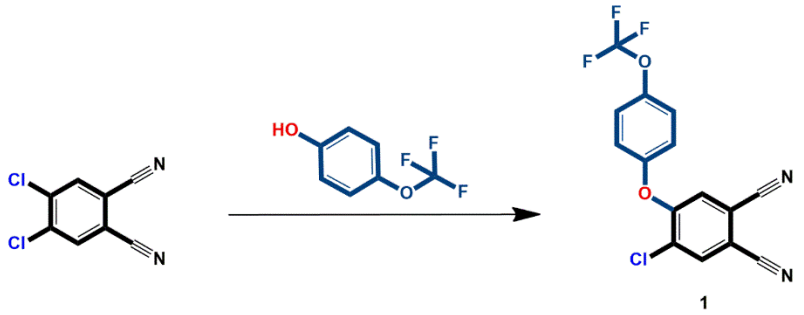

Scheme 1. The synthetic pathway for phthalonitrile (**1**): DMF, potassium carbonate, room temperature, 48 hours.

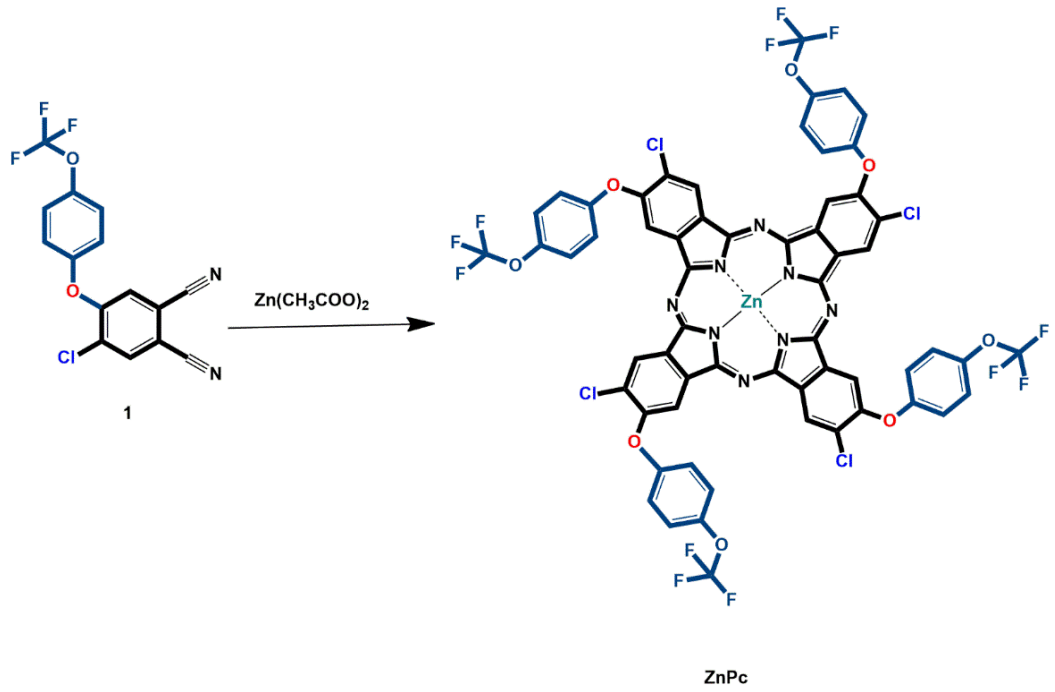

Scheme 2. The synthetic route for zinc (II) phthalocyanine derivative (ZnPc); DMAE, reflux temperature, 24 hours.

(aromatic), C≡N (nitrile), CF_3, and C-O-C, respectively [6,11,16].

The synthetic route for phthalonitrile (1) and its zinc (II) phthalocyanine derivative (ZnPc) is demonstrated in Scheme 2. Cyclotetramerization of phthalonitrile 1 in the presence of the metal ion resulted in the preparation of a macromolecule (ZnPc) that, in turn, was purified by applying column chromatography. The product was characterized using FT-IR, UV-vis, and ^{1}H NMR spectroscopic techniques. The obtained data confirmed the synthesis of the target structure. In the ^{1}H NMR spectrum of macromolecule ZnPc, the aromatic protons of the phthalonitrile were observed at 8.10 (1H) and 7.78 (1H) as singlets, whereas those of the 4-trifluoromethoxyphenyl group appeared at around 7.60-7.55 (2H) and 7.35-7.31 (2H) as broad doublets. A shift in the chemical shift of the protons, which are neighbors of the -CN group, appeared in the ^{1}H NMR spectrum of ZnPc, which is expected due to the change in the environment of the mentioned hydrogens. In the FT-IR spectrum, the disappearance of the signal for the C≡N group at 2259 demonstrated the formation of cyclotetramerization of phthalonitrile 1. Also, the bands appearing at 3069, 1379, and 1082 cm^{-1} corresponded to C-H (aromatic), C-F, and C-O-C, respectively [6,11,16].

Generally, the mass spectra of the studied compound are assigned to the ionized intact phthalocyanines; however, some differences may arise from the medium (matrix

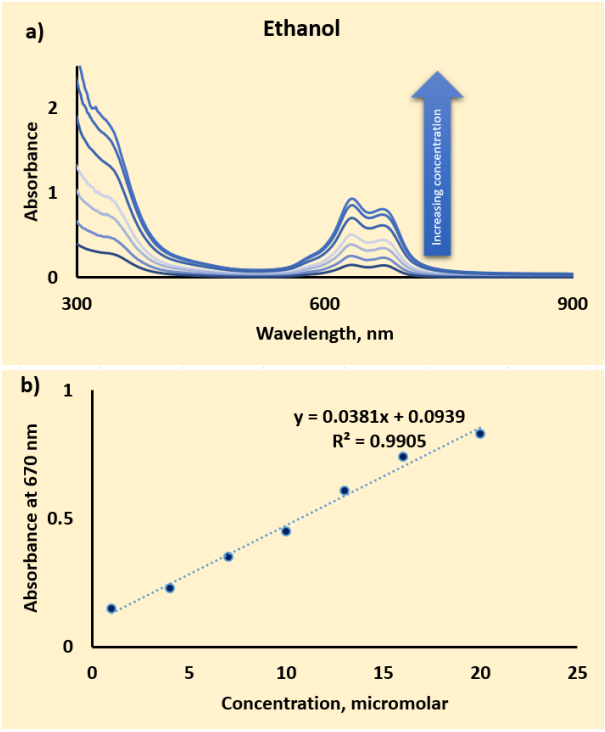

Figure 1. (a) The electronic absorption spectra of macromolecule (ZnPc) at different concentrations (1-20 micromolar) in ethanol; (b) The absorbance-concentration plot of ZnPc.

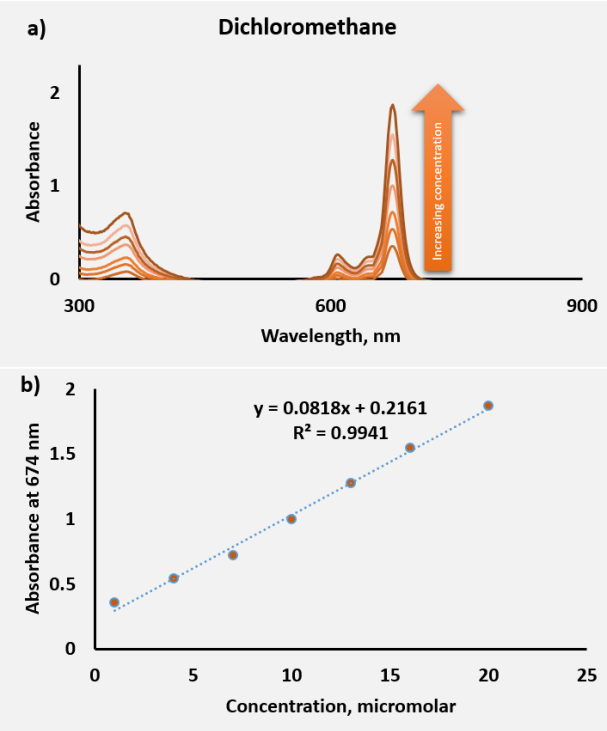

Figure 2. The electronic absorption spectra of macromolecule (ZnPc) at different concentrations (1-20 micromolar) in dichloromethane; (b) The absorbance-concentration plot of ZnPc.

nature, basicity (e.g., potassium hydroxide)/acidity (e.g., acetic acid), H_2O, or moisture in which the measurement is performed. Some of these differences have been reported in the literature [17,18]. In the MALDI-TOF spectrum of macromolecule ZnPc, the molecular ion peak observed at 1437.39 m/z was assigned to $[M + OH]^+$. In addition, the electronic absorption spectra of the product in different solvents (Table 1) yielded two characteristic bands in the ultraviolet (339-354 nm) and visible (670-677 nm) regions.

3.2 Aggregation Studies

Solubility significantly affects the application of phthalocyanines in various fields. Indeed, π- π stacking between phthalocyanine rings leads to aggregation, thereby limiting their solubility. Besides, aggregation plays a vital role in the bioavailability, singlet oxygen production efficiency, *in vivo* distribution, and PDT properties [19]. The introduction of substituents and metal ions into the phthalocyanine rings can overcome remarkable aggregation and low solubility. Additionally, temperature, concentration, and solvent are factors influencing aggregation. Generally, studying the electronic absorption spectra of phthalocyanines at various concentrations is a suitable method for evaluating

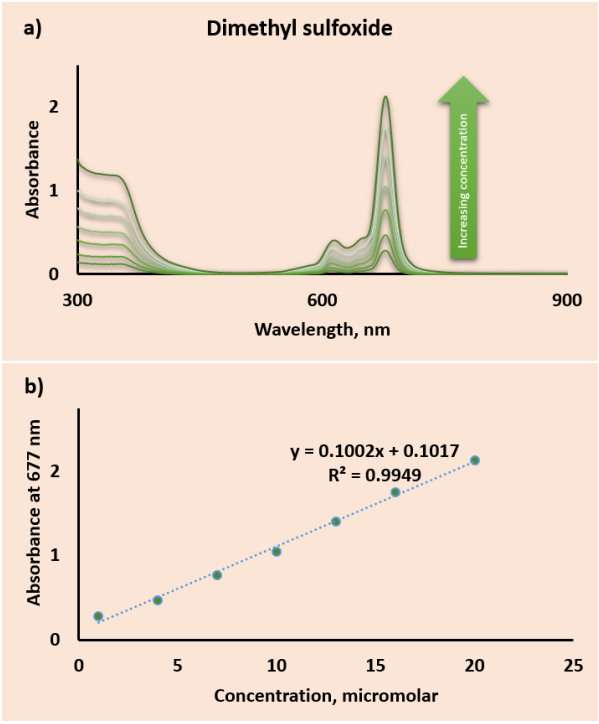

Figure 3. (a) The electronic absorption spectra of macromolecule (ZnPc) at different concentrations (1-20 micromolar) in dimethyl sulfoxide; (b) The absorbance-concentration plot of ZnPc.

aggregates and their control. The UV-vis spectrum of a phthalocyanine includes two characteristic bands: (a) the Q-band corresponds to π-π* transition from the highest occupied molecular orbital (HOMO) to the lowest unoccupied molecular orbital (LUMO) of the phthalocyanine ring and appears in the visible region (650-750 nm), (b) the B-band is assigned to deeper π-π* transitions [1,2,6,7]. Metal ions, substituents, and the symmetry of π-conjugated systems can affect the band position and width [20-25].

In this study, the concentration effect (1-20 micromolar) on the aggregation of the zinc (II) phthalocyanine was studied in three different solvents: ethanol, DCM, and DMSO. The recorded spectra are demonstrated in Figures 1-3. The results obtained are summarized in Table 1. Regardless of the solvent nature, an increase in the concentration of macromolecule (ZnPc) was followed by an increase in the intensity of Q-band without observation of any new band. As a result, the zinc (II) phthalocyanine obeyed the Lambert–Beer law in all the solvents at the studied concentration range (1-20 μM). Moreover, the Q band shifted to longer wavelengths as the solvent's refractive index increased in the following order: ethanol < DCM < DMSO. The results obtained by applying the Bayliss method [16] (Figure 4) confirmed a linear relationship between the Q-band frequency and the solvent refractive index. Therefore, the red shift of the Q-band mainly corresponded to the solvation effect.

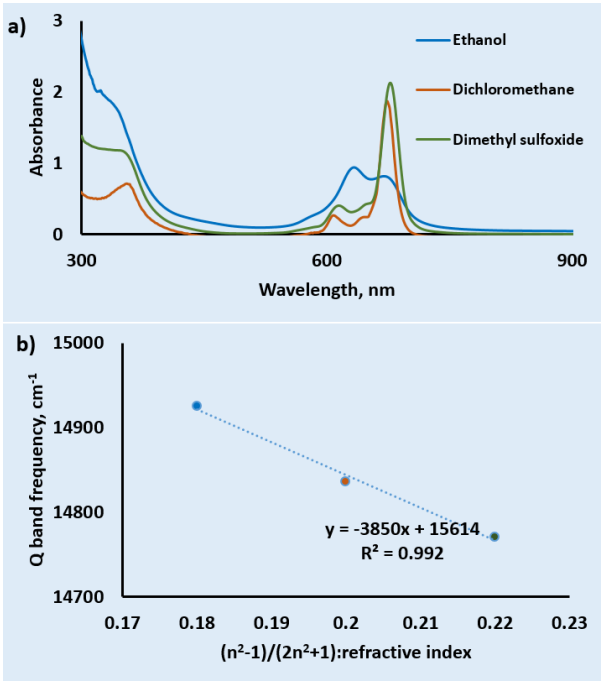

Figure 4. The UV-vis spectra of macromolecule (ZnPc) in different solvents (concentration; 20 micromolar), (d) Plot of the Q band frequency of macromolecule (ZnPc) against $(n^2 - 1)/(2n^2 + 1)$.

3.3 Singlet oxygen quantum yield

As the drugs used in chemotherapy can kill healthy cells as well as cancer cells, the development of this method has been limited, and an urgent alternative approach should be designed. Photodynamic therapy has recently attracted attention in cancer treatment. Light, a photosensitizing compound, and an oxygen molecule are the three main parts of this technique. In this method, the photosensitizer is activated by light exposure and then converts triplet oxygen to its singlet form, which can attack cancer cells. Therefore, the ϕ_Δ value of a photosensitizing agent can serve as a useful parameter for assessing its anticancer performance [16,26]. In this study, the ϕ_Δ value of macromolecule (ZnPc) was calculated by applying the phosphorescence signal of singlet oxygen at 1206 nm [15]. The ϕ_Δ value was determined to be 0.81, which was higher than that of the unsubstituted zinc (II) phthalocyanine (ϕ_Δ = 0.67). Indeed, chlorine, as an electron-withdrawing atom in the phthalocyanine ring, may lower the energy gap and, in turn, improve the optical properties [27].

Table 1. The data of UV-vis spectra of macromolecule (ZnPc).

Solvent	B-band (nm)	Log ε of B-band	Q-band (nm)	Log ε of Q-band
Ethanol	335	4.97	670	4.61
Dichloromethane	354	4.55	674	4.97
Dimethyl sulfoxide	339	4.77	677	5.02

4. Conclusion

This study reports the successful preparation of a new phthalonitrile derivative bearing a chlorine atom and a fluorinated phenoxy group. The resultant compound was cyclotetramerized in the presence of the corresponding metal cation to afford the peripherally octa-substituted zinc (II) phthalocyanine via a one-step template mechanism. The electronic absorption spectra of the newly synthesized phthalocyanine were recorded at concentrations ranging from 1 to 20 µM in ethanol, dichloromethane, and dimethyl sulfoxide to assess the effects of concentration and solvent on aggregation. Moreover, the singlet oxygen generation ability of the zinc (II) phthalocyanine (ZnPc) was determined to be 0.81. This compound exhibited higher singlet oxygen generation capacity than the reference. As a result, the photochemical and photodegradation properties of the newly synthesized phthalocyanine can be studied to measure its probable photosensitizing efficiency for photodynamic therapeutic applications.

Author's Contributions

Nazlı Farajzadeh Öztürk: Drafted and wrote the manuscript, performed the experiment and result analysis.

Sevgi Sarıgül Özbek: Assisted in analytical analysis on the structure, result interpretation, and helped in manuscript preparation.

Ethics

The authors declare no ethical concerns related to this study.

There are no ethical issues after the publication of this manuscript.

References

[1]. Zhang, S, Yang, N, et al. 2026. Detachable Fluorinated Phthalocyanine Aggregates for Carrier-Free PDT: Effect of Axial Symmetry on Dynamic Morphological Adjustment and Photodynamic Efficiency. *Advanced Functional Materials*; 36(6): e13920.

[2]. Wang, S -R, Yao, Y, et al. 2022. Intra-ring proton transfer effect on the Structure-NLO property relationships of phthalocyanine derivatives. *Journal of Molecular Liquids*; 368: 120652.

[3]. Peng, J, Li, X, et al. 2022. Photoelectrochemical sensor based on zinc phthalocyanine semiconducting polymer dots for ultrasensitive detection of dopamine. *Sensors & Actuators: B. Chemical*; 360: 131619.

[4]. Lu, C, Dai, Q, et al. 2023. Towards high photoresponse of perovskite nanowire/copper phthalocyanine heterostructured photodetector. *Nanotechnology*; 34: 495201.

[5]. Li, X, Wu, X, et al. 2021. Promoting Oxygen Reduction Reaction by InducingOut-of-Plane Polarization in a Metal Phthalocyanine Catalyst. *Advanced Materials*; 35: 2302467.

[6]. Karaoğlu, HP, Sağlam Ö, et al. 2021. Novel symmetrical and unsymmetrical fluorine-containing metallophthalocyanines: synthesis, characterization and investigation of their biological properties. *Dalton Transactions*; 50: 9700-9708.

[7]. Revuelta-Maza, M, González-Jiméne, P, et al. 2020. Fluorine-substituted tetracationic ABAB-phthalocyanines for efficient photodynamic inactivation of Gram-positive and Gram-negative bacteria. *European Journal of Medicinal Chemistry*; 187: 111957.

[8]. Özcan, S, Kobak, RZ, et al. 2022. Synthesis, Electrochemistry, Spectroelectrochemistry, and Electrochromism of Metallophthalocyanines Substituted with Four (2,4,5-Trimethylphenyl)ethynyl Groups. *Electroanalysis*; 34(10): 1610-1620.

[9]. Dyrda, GM, Pędziński T. 2025. Photostability of Indium Phthalocyanines in Organic Solvents. *Colorants*; 4(1):4.

[10]. Erdem, M, Korkmaz, E, et al. 2021. Nonlinear optical behavior and optical power limiting characteristics of peripheral symmetrical and non-symmetrical zinc phthalocyanines with nanosecond pulsed excitation. *Polyhedron*; 195: 114975.

[11]. Karaoğlu, HP, Sağlam, Ö, et al. 2021. Novel symmetrical and unsymmetrical fluorine-containing metallophthalocyanines: synthesis, characterization and investigation of their biological properties. *Dalton Transactions*; 50: 9700–9708.

[12]. Johnson, PI, Gregory, GN, et al. 2024. Thermodynamic implications of size, hydrophilicity, andfluorine content on perfluoroalkyl adsorption in NU-1000. *AIChE Journal*; 70: e18579.

[13]. Liu, Z, Qin, L, et al. 2021. Improving stability and reversibility via fluorine doping in aqueous zinc–manganese batteries. *Materials Today Energy*; 22: 100851.

[14]. Handa, M, Yomoto, T, et al. 2025. Syntheses, structures and properties of a phthalocyanine peripherally introduced with bis(3,5-trifluoromethyl)phenyl substituents and its zinc(II) and cobalt(II) complexes. *Journal of Porphyrins and Phthalocyanines*; 29: 1219–1230.

[15]. Farajzadeh, N, Kuşçulu, NG, et al. 2022. Anticancer activity of novel silicon phthalocyanines against the colorectal adenocarcinoma cell line (DLD-1). *New Journal of Chemistry*; 46: 19863–19873.

[16]. Farajzadeh, N, Akyüz, D, 2020. Synthesis, electrochemistry and in situ spectroelectrochemistry of novel tetra- and octa-substituted

metallophthalocyanines bearing peripherally 4-(trifluoromethoxy)phenoxy groups. *Polyhedron*; 177: 114264.

[17]. Srinivasan, N, Haney, CA, et al. 1999. Investigation of MALDI-TOF Mass Spectrometry of Diverse Synthetic Metalloporphyrins, Phthalocyanines and Multiporphyrin Arrays. Journal of Porphyrins and Phthalocyanines; 3: 283–291.

[18]. Günsel, A, Kandaz, M, et al B. 2011. Peripheral and non-peripheral-designed multifunctional phthalocyanines; synthesis, electrochemistry, spectroelectrochemistry and metal ion binding studies. *Polyhedron*; 30: 1446–1455.

[19]. Xiong, J, Xue, EY, Ng, DKP, 2023. Synthesis, Cellular Uptake, and Photodynamic Activity of Oligogalactosyl Zinc(II) Phthalocyanines. *ChemPlusChem*; 88(2): e202200285.

[20]. Göller, İ, Yenilmez, HY, Öztürk, NF, 2024. Biological properties of 4-trifluoromethylbenzyloxy-substituted cobalt phthalocyanine-gold nanoparticle conjugates. *Applied Organometallic Chemistry*; 38(7): e7505.

[21]. Kaplan, E, Karazehir, T, et al. 2023. Peripherally and non-peripherally carboxylic acid substituted Cu(II) phthalocyanine/reduced graphene oxide nanohybrids for hydrogen evolution reaction catalysts. Molecular Systems Design & Engineering; 8: 810-821.

[22]. Demir, F, Yenilmez, HY, et al. 2022. Synthesis, electrochemistry, and electrocatalytic activity of thiazole-substituted phthalocyanine complexes. Journal of Solid State Electrochemistry; 26: 761–772.

[23]. Sağlam, Ö, Farajzadeh, N, et al. 2021. Effect of Position and Connected Atom on Photophysical and Photochemical Properties of Some Fluorinated Metallophthalocyanines. Photochemistry and Photobiology; 97(2): 270-277.

[24]. Yurttaş, AG, Sevim, AM, et al. 2022. The effects of zinc(II)phthalocyanine photosensitizers on biological activities of epitheloid cervix carcinoma cells and precise determination of absorbed fluence at a specific Wavelength. Dyes and Pigments; 198: 110012.

[25]. Özçeşmeci, M, Isik, S, et al. 2026. PEGylated isothiocyanate-functionalized zinc(II) phthalocyanine exhibits cell-type dependent photodynamic activity in 2D and 3D tumor models. *Journal of Photochemistry and Photobiology B: Biology*; 275, 113354.

[26]. Yenilmez, HY, Farajzadeh, N, et al. 2023. Effect of axial ligand length on biological and anticancer properties of axially disubstituted silicon phthalocyanines. *Chemistry & Biodiversity*; 20(4): e202201167.

[27]. Jothi, AI, Rajarathinam, C, et al. 2022. Substituent effects on the mesogenic benzylidenes of 4-methylaniline: synthesis, characterization, DFT, NLO, photophysical, molecular docking, and antibacterial studies. *Journal of Molecular Liquids*; 347: 117980.